www.rericjournal.ait.ac.th

Analysis on Optimal Thermohydraulic Performance of Solar Air Heater Having Multiple V-shaped Wire Rib Roughness on Absorber Plate

Dhananjay Kumar*[1] and Laljee Prasad*

Abstract –*The use of artificial roughness on the underside of the absorber plate is an effective and economic way to enhance the heat transfer from the collector to the air in a solar air heater duct. This paper presents the analysis on thermal and thermohydraulic efficiency also called "effective efficiency" of solar air heater having multiple v-shaped wire rib roughness underside of the absorber plate. The mathematical equations are analytically derived and solved by developing a computer program in MATLAB code in order to analyze the effect of various ambient, operating and design parameters on the thermal efficiency and effective efficiency (based on the net gain after taking account of the pumping power) of such air heaters. The study shows substantial enhancement in thermal efficiency over solar air heater with plane ones. The thermal efficiency enhancement is also accompanied by a considerable increase in the pumping power requirement due the increase in the friction factor. The optimum design and operating conditions have been determined on the basis of thermohydraulic considerations. It has been found that, the systems operating in a specified range of Reynolds number shows better thermohydraulic performance depending upon the insolation. A relationship between system and operating parameters that combine to yield optimum performance has been developed.*

Keywords – artificial roughness, Reynolds's number, relative roughness height, relative roughness pitch, solar air heater.

1. INTRODUCTION

The conventional solar air heater is a flat plate collector consisting of an absorber plate, a transparent covers at the top and insulation at the bottom and on the sides. Schematic diagram of conventional solar air heater is shown in Figure 1. The incident solar radiation is absorbed by the absorber plate and converted into thermal energy. These find several applications like space heating, crop drying, seasoning of timbers, cooking as well as curing of industrial products etc. The thermal efficiency of solar air heater is poor because the low rate of heat transfers capability between air and absorber plate, In order to make a solar air heater is economically viable and more effective in solar energy utilization system, thermal efficiency needs to be improved by enhancing the rate of heat transfer capability between absorber plate and air flowing in the duct. The attempts adopted to enhance the rate of heat transfer include provision of artificial roughness in the form of repeated ribs underside of the absorber plate. The use of artificial roughness on a surface is an effective and economic way for enhance the rate of heat transfer to fluid flowing in a duct [1].

Turbulence promoters or small height element have been used to improve the convective heat transfer coefficient between the absorber plate and air flowing in the duct, by creating turbulence. However, there is substantial increase in the frictional losses and hence, greater power requirement by fan or blower. In order to keep the friction losses at a minimum level, the turbulence must be created only in the region very close to the heat-transferring surface to break laminar sub-layer for improving the heat transfer. This is done by keeping the height of the roughness elements small in comparison to the duct dimension [2]. The surface roughness can be produced by various methods, such as casting, forming, machining, sand blasting, welding ribs and by fixing thin circular wires along the surfaces. The application of artificial roughness in solar air heater owes its origin to several investigations [3-6] carried out in connection with the improvement of heat transfer in nuclear reactors and turbine blades. Several investigations have been carried out to study the effect of artificial roughness on heat transfer and friction factor for two opposite roughened surfaces by Han [7], Han *et al*. [8], Wright *et al*. [9], Han and Park [6], Taslim *et al*. [10], [11] and Gao *et al.* [12] also developed the correlations. The provision of artificial roughness underside on the absorber plate could substantially enhance the heat transfer capability of solar air heater. Prasad and Mullick [13] utilized artificial roughness in the form of small height protruding wire to increase the heat transfer coefficients for drying purpose. Prasad and Saini [14] investigated fully developed turbulent flow in a solar air heater duct with a small diameter transverse wire rib roughness on the absorber plate they also applied wall similarity law and reproduced the heat transfer and friction factor correlations as developed by [1] and [7]. Deo *et al*. [15] investigated the effect of relative roughness height, angle of attack on heat transfer and friction factor for multigap v-down ribs combined with staggered ribs they find thermohydraulic performance on the basis of methods adopted by [25]. They also developed the correlations that relate the system and operating parameters. Karmare and Tikekar

*Department of Mechanical Engineering, National Institute of Technology, Jamshedpur, Jharkhand-831014, India.

[1] Corresponding author;
Tel: +919430818748.
E-mail: dhananjaykumar84nit@gmail.com.

[16] experimentally investigated the optimal thermohydraulic performance of solar air heater with metal rib grits roughness underside the absorber plate and presented the correlations for Nusselt number and friction factor for optimal performance condition. Karwa *et al*. [17] used chamfered rib roughness on the absorber plate and they found that the solar air heater having higher relative roughness height of the roughness elements yields a better performance. Saini and Saini [24] studied the effect of arc shaped ribs on the heat transfer coefficient and friction factor of rectangular ducts. Momin *et al.* [19] investigated the effect of v-shaped rib roughness on the absorber plate and they found that maximum thermohydraulic performance occurred for an angle of attack of 60°. Prasad *et al.* [20], [21] optimized the thermohydraulic performance of three sides artificially roughened solar air heater with transverse wire rib roughness on the absorber plate and developed the correlations for Stanton number and friction factor. Gupta *et al.* [30] established the optimum design parameters under actual climatic conditions for roughened solar air heater on the basis of thermohydraulic considerations. It has been found that the effective efficiency of a roughened solar air heater increases as the insolation increases for Reynolds numbers higher than 10,000. However, at lower Reynolds numbers ($Re < 10{,}000$) the thermohydraulic efficiency decreases with increasing insolation. Singh *et al*. [31] experimentally investigated the performance of rectangular ducts with v-down ribs having symmetrical gap equal to rib height at the centre of both legs on one broad wall. They observed that the friction factor and Nusselt number are strong function of flow-attack-angle. Kumar *et al*. [32] developed the correlation for Nusselt number and friction factor for rectangular duct solar air heater having multi v-shaped rib with gap roughness on principal wall. Karwa and Chitoshiya [33] experimentally investigated the results on thermo-hydraulic performance of solar air heater with 60° v-down discrete rib roughness on the air flow side of the absorber plate using mathematical model. Typical values of system and operating parameters are used in the present investigation, have been shown in Table 1.

The main objectives of the present investigation are:

1. To study the effect of relative roughness height (e/D), angle of attack (α) insolation (I) and mass flow rate ($\dot{m}$) in terms of Reynolds number (Re) values on thermohydraulic performance of solar air heater roughened with multiple v-shaped wire ribs and compare with the values obtained using smooth duct.
2. To find the effective efficiency of a roughened solar air heater has an optimum value corresponding to a certain Reynolds number and specific values of operating and geometrical conditions.
3. To compare the effective efficiency of proposed roughness pattern multiple v-shaped and other best performing variations of the rib roughness as reported by other researchers in the recent and past.

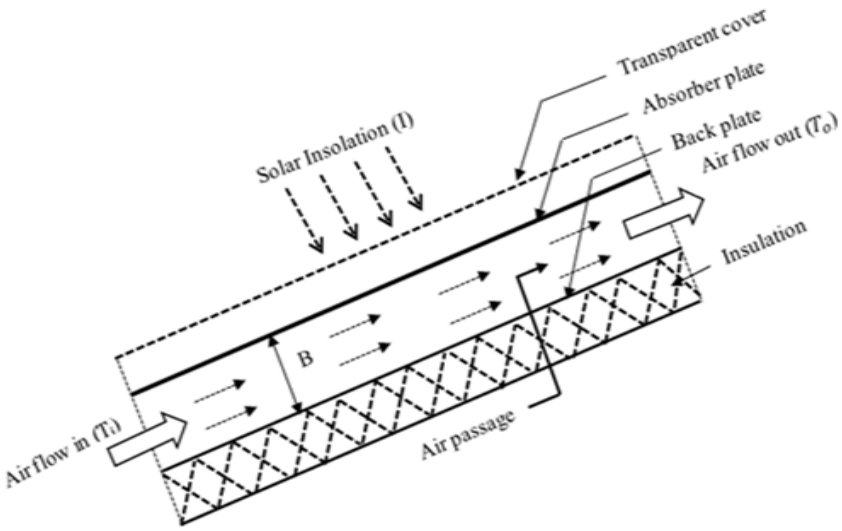

Fig. 1. Schematic diagram of conventional solar air heater.

2. PERFORMANCE ANALYSIS OF SOLAR AIR HEATER

The effective efficiency (η_{eff}) of solar collector is defined as the ratio of net thermal energy gain to the input thermal energy and is given by Cortes and Piacentini [25].

$$\eta_{eff} = \left[\frac{(Q_u - P_m/\zeta)}{IA_c}\right] \quad (1)$$

Where $\zeta = \eta_f\eta_m\eta_{tr}\eta_{th}$ is a factor that accounts for conversion of mechanical energy or pumping power into equivalent thermal energy.

The rate of useful thermal energy gain is calculated from the equation:

$$Q_u = F'A_c[I\,(\tau\alpha)_e - U_L(T_o - T_i)/2] \quad (2)$$

Where $F' = [h/(h + U_L]$ (3)

In order to evaluate thermal performance of solar air heater, Equation 1 can be expressed in a more usable form by introducing the term 'collector heat-removal factor' F_R Hottel-Whillier-Bliss equation reported by Duffie and Beckman [26].

$$Q_u = F_R A_c[I\,(\tau\alpha)_e - U_L(T_i - T_a)] \quad (4)$$

In a particular case, when the solar air heaters draw air at ambient temperature (*i.e.* $T_i = T_a$), the useful heat gain of a solar air heater is given by [27]:

$$Q_u = F_R A_c[I(\tau\alpha)_e - U_L(T_o - T_i)] \quad (5)$$

Where F_R the collector heat-removal factor is referred to outlet air temperature and is given by:

$$F_R = \frac{\dot{m}C_p}{A_c U_L}\left[1 - \exp^{-}\left\{\frac{F'U_L A_c}{\dot{m}C_p}\right\}\right] \quad (6)$$

The rate of useful energy gain in a solar air heater may also be calculated from the following equations:

$$Q_u = \dot{m}C_p(T_o - T_i) = h\,A_c(\overline{T}_p - \overline{T}_f) \quad (7)$$

The mechanical power consumed is given by the expression:

$$P_m = \frac{\dot{m}(\Delta P)_d}{\rho} \quad (8)$$

Where $(\Delta P)_d = \frac{(4fLV^2\rho)}{2D}$ (9)

Where equivalent diameter D of the duct is given by:

$$D = \frac{4WB}{2(W + B)} \quad (10)$$

The thermal efficiency of solar air heater can be expressed by the following equation:

$$\eta_{th} = \frac{Q_u}{IA_c} = F_R\left[(\tau\alpha)_e - U_L\left(\frac{T_i - T_a}{I}\right)\right] \quad (11)$$

In order to find the value of heat transfer coefficient for smooth solar air heater duct,

Dittus –Boelter equation was used [15]:

$$h_s = 0.023(k/D)(Re)^{0.8}Pr^{0.4} \quad (12)$$

The friction factor (f_s) for smooth solar air heater is given by Blasius equation [15]:

$$f_s = 0.085\,(Re)^{-0.25} \quad (13)$$

The heat transfer coefficient (h) between the absorber plate and the air flowing over it, is calculated from:

$$h = \frac{(K.Nu)}{D} \quad (14)$$

Heat transfer coefficient for multiple v- shaped wire rib roughened solar air heater duct can be calculated using the equation, given below [28]:

$$Nu_r = 3.35x10^{-5}\,Re^{0.92}\,(e/D)^{0.77}\left(\frac{W}{w}\right)^{0.43} (\alpha/90^{\circ})^{-0.49}\exp^{[-0.61(Ln(\alpha/90))^2]} \exp^{[-0.1177(Ln(W/w))^2]}\,(P/e)^{8.54} \exp^{[-2.0407(Ln(P/e))^2]} \quad (15)$$

The friction factor (f_r) for roughened solar air heater is given by [28]:

$$f_r = 4.47x10^{-4}\,Re^{-0.3188}\,(e/D)^{0.73}\left(\frac{W}{w}\right)^{0.22} (\alpha/90^{\circ})^{-0.39}\exp^{[-0.52(Ln(\alpha/90))^2]} \exp^{[-2.133(Ln(P/e))^2]}\,(P/e)^{8.9} \quad (16)$$

The overall heat loss coefficient (U_L) of a solar air heater is the sum of the top loss coefficient (U_t), bottom loss coefficient (U_b), and side loss coefficient (U_s) and is given by:

$$U_L = U_t + U_b + U_s \quad (17)$$

The top loss coefficient (U_t) is evaluated by using the equation as proposed by [29]:

$$U_t = \left[\frac{N}{\left(\frac{C}{\overline{T}_p}\right)\left(\frac{\overline{T}_p - T_a}{N + f'}\right)^{0.252}} + \frac{1}{h_w}\right]^{-1} + \left[\frac{\sigma(\overline{T}_p^2 + T_a^2)(\overline{T}_p + T_a)}{\frac{1}{\varepsilon_p + 0.0425N(1-\varepsilon_p)} + \frac{(2N + f' - 1)}{\varepsilon_g} - N}\right] \quad (18)$$

Where

$$C = 204.429\,((\cos\beta)^{0.252}/\,(L_1)^{0.24}) \quad (19)$$

$$f' = \left(\left(\frac{9}{h_w}\right) - \left(\frac{30}{h_w^2}\right)\right)\left(\frac{T_a}{316.9}\right)(1 + 0.091N) \quad (20)$$

and

$$h_w = 5.7 + 3.8V_w \quad (21)$$

The bottom heat loss coefficient (U_b) is calculated using the relation given below:

$$U_b = \frac{K_i}{\delta_i} \quad (22)$$

The side heat loss coefficient (U_s) is calculated using the relation given by:

$$U_s = \frac{(L + W)BK_i}{LW\delta_i} \quad (23)$$

Roughness Reynolds number (e^+) is calculated using the relation given below [18]:

$$e^+ = (e/D)\sqrt{\frac{f_r}{2}}\,Re \quad (24)$$

Reynolds number (Re) is calculated by:

$$Re = \frac{(G.D)}{\mu} \quad (25)$$

Where mass velocity of air (G) is calculating using the relation given below:

$$G = \frac{\dot{m}}{(W.B)} \quad (26)$$

and mass flow rate of air ($\dot{m}$) is calculated by:

$$\dot{m} = \frac{Q_u}{(C_p.\Delta T)} \quad (27)$$

The enhancement ratio (E_R) is the ratio of effective efficiencies of one side roughened solar air heater to the four side smooth absorber plate solar air heater.

$$E_R = \left[\frac{(\text{Effective efficiency})_{\text{Rough}}}{(\text{Effective efficiency})_{\text{Smooth}}}\right] \quad (28)$$

Nikuradse [18] defined and developed the theory for roughened surfaces fluid flow in three regions (laminar, turbulent and fully developed turbulent flow) based on the values of roughness Reynolds number (e^+) which is calculated by the Equation 24. The three regions are:-

(i) Laminar region

In the first region, the roughness has no effect on the resistance for low Reynolds numbers. This range includes complete laminar flow and measured pressure loss data are correlated by Nikuradse [18] in the form of R (e^+) as under

$$(0 < e^+ < 5)$$

$$R(e^+) = 5.5 + 2.5 \ln (e^+) \quad (29)$$

(ii) Transition region

The second region is called the transition zone; the effect of roughness height becomes noticeable to a greater degree. The resistance increases with increase in roughness Reynolds number (e^+). The resistance depends on the Reynolds number as well as on the relative roughness height.

$$(5 \le e^+ \le 70) \quad (30)$$

(iii) Fully rough region

The third region is called the fully developed turbulent region, the resistance due to roughness was found to be independent of the roughness Reynolds number and it attains a constant value. It follows the quadratic law of resistance.

$$e^+ > 70 \quad (31)$$

3. SYSTEM AND OPERATING PARAMETERS FOR ARTIFICIALLY ROUGHENED SOLAR AIR HEATER DUCT

The solar air heater duct is simply a thin metallic sheet that consists of multiple v-shaped wires as the roughness elements fixed on its flow sides of the absorber plate as shown in Figure 2. In order to evaluate thermohydraulic performance of roughened solar air heater ducts, values of system and operating parameters were selected as given in Table 1.

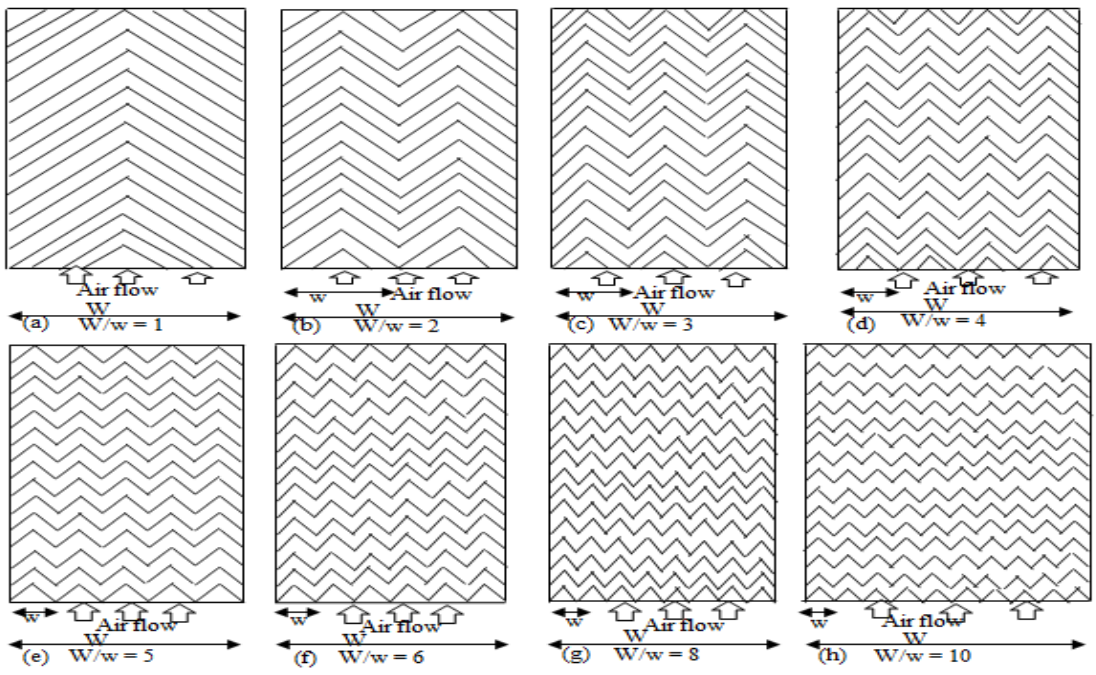

Fig. 2. Multiple V-shape wires roughness geometry on absorber plate.

Table 1. **Typical values of system and operating parameters employed for computation of effective efficiency of solar air heaters.**

System Parameters	
Length of absorber plate (L), m	1.5
Width of absorber plate (W), m	1.0
Duct height (B), m	0.025
Air gap between absorber plate and glass cover (L_1), m	0.04
Thickness of glass cover (L_g), m	0.004
Thermal conductivity of glass (K_g), W/mK	0.75
Thickness of insulation (δ_i), m	0.05
Thermal conductivity of insulation (K_i), W/mK	0.037
Number of glass cover (N), dimensionless	1
Effective transmittance absorptance product $(\tau\alpha)_e$, dimensionless	0.84
Emissivity of absorber plate (ε_p), dimensionless	0.9
Emissivity of glass cover (ε_g), dimensionless	0.88
Thickness of collector edge (L_e), m	0.2
Relative roughness height (e/D), dimensionless	0.0205 - 0.0410
Relative roughness pitch (P/e), dimensionless	10
Angle of attack (α), dimensionless	30 - 75°
Reynolds number (Re), dimensionless	2500-25000
Operating Parameters	
Ambient temperature (T_a), K	300
Wind velocity (V_w), m/s	1.2
Temperature rise parameters ($\Delta T/I$), $°Cm^2/W$	0.0025 - 0.010
Intensity of solar radiation or insolation (I), W/m^2	500 - 1200

4. RESULTS AND DISCUSSION

A mathematical approach for solar air heater ducts and their system and operating parameters, various design have been plots (Figures 3 –15). The performance evaluation has also been carried out to explore the effect of relative roughness height (e/D), relative roughness width (W/w), angle of attack (α), and solar insolation (I) on thermal and effective efficiency for multiple v-shaped roughened and smooth absorber plate solar air heaters. Figure 3(a) shows the variation of useful heat gain (Q_u) and pumping power (P_m/ζ) of the fan for multiple v-shaped wires rib roughened solar air heater as a function of Reynolds number (Re). It is found that the rate of increase of useful energy gain is comparatively higher for lower range of Reynolds number (Re < 15,500 approx.) whereas this rate of increase is lower at higher range of Reynolds number. The rate of increase of power consumption is low for lower range of Reynolds number (Re < 15,500 approx.) and increases comparatively with faster rate in higher range of Reynolds number. This variation indicates the trend as expected. Figure 3(b) shows the comparison of variations of useful heat gain (Q_u) and pumping power (P_m/ζ) for multiple v-shaped wire rib roughened and smooth absorber plate solar air heaters with Reynolds number (Re). It is clear that the rate of increase of useful energy gain is relatively higher at lower range of Reynolds number, whereas it is a bit lower at higher range of Reynolds number. But power consumption at the lower Reynolds number (Re < 13,000 approx.) remains almost same for both rough and smooth solar air heaters, and after this value of Reynolds number it increases rapidly, however the power consumption is more than that of the smooth solar air heaters in this range of Reynolds number. The power consumption does not exceed the rate of useful energy gain, i.e. the net energy gain rate is positive and it is also clear that at higher Reynolds number, the rate of useful energy collected becomes almost constant but the power consumption rises steeply.

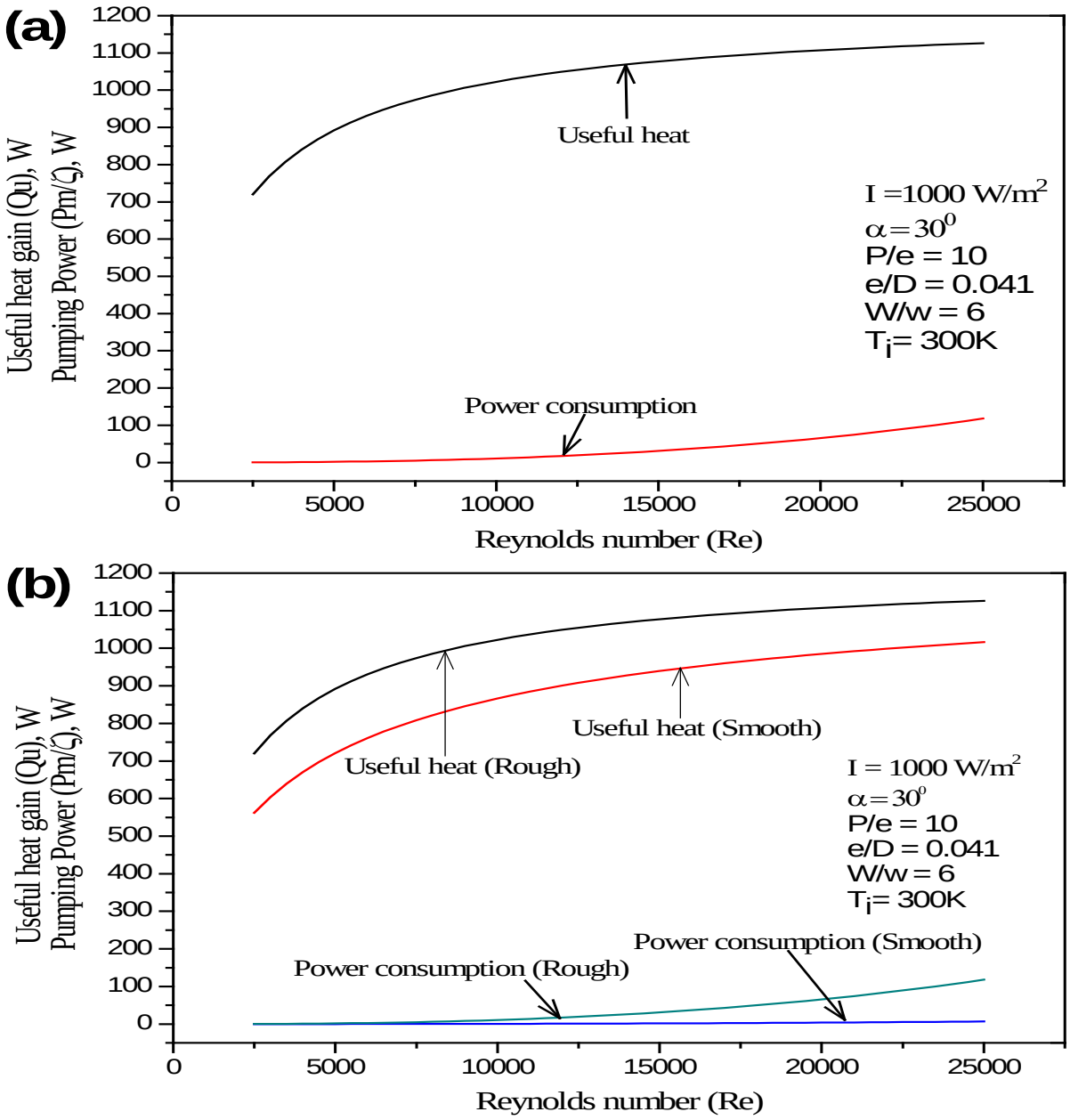

Fig. 3. (a) Energy balance for roughened solar air heater (b) Comparison of energy-balance for smooth and roughened solar air heater.

4.1. Effect of Relative Roughness Height (e/D)

The variation in effective efficiency with Reynolds number at different values of relative roughness height (e/D = 0.020, 0.026, 0.032 and 0.041) for fixed value of relative roughness width (W/w = 6), relative roughness pitch (P/e = 10) and angle of attack (α= 〚30〛^°) at insolation (I) of 1000 W/m2 and 500 W/m2 have been shown in Figures 4 (a) and (b), respectively.

It is found that from Figure 4(a) the Reynolds number increases, the effective efficiency increases, attains a maximum at certain value of Reynolds number, and then decreases with further increase in Reynolds number. At higher value of relative roughness height the effective efficiency is higher and at lower value of relative roughness height it is lower. Similar trends of variations are obtained for both values of insolation however, at lower values of insolation (I= 500 W/m^2), the effective efficiency, after attaining its maximum value, decreases faster rate with respect to (I= 1000 W/m^2). Thus there exists an optimum value of effective efficiency for a given roughness configuration. This effect shows that the Reynolds number is a strong parameter that affects the pumping power and thermal energy gain, thereby affecting the effective efficiency.

In order to investigate the behaviour of relative roughness height on effective efficiency of solar collector, the parameters are taken to be fixed values of relative roughness pitch (P/e), relative roughness width (W/w), insolation (I) and angle of attack(α) as shown in Figure 4(b). It is found that the best thermohydraulic performance is at relative roughness height (e/D) = 0.041 and Reynolds number (Re) = 13,500 as indicated in Figure 4(b). This fact is possible at higher height of roughness create more turbulence to the flow of air inside the duct, resulting in higher rate of heat transfer as compared to smaller height of roughness.

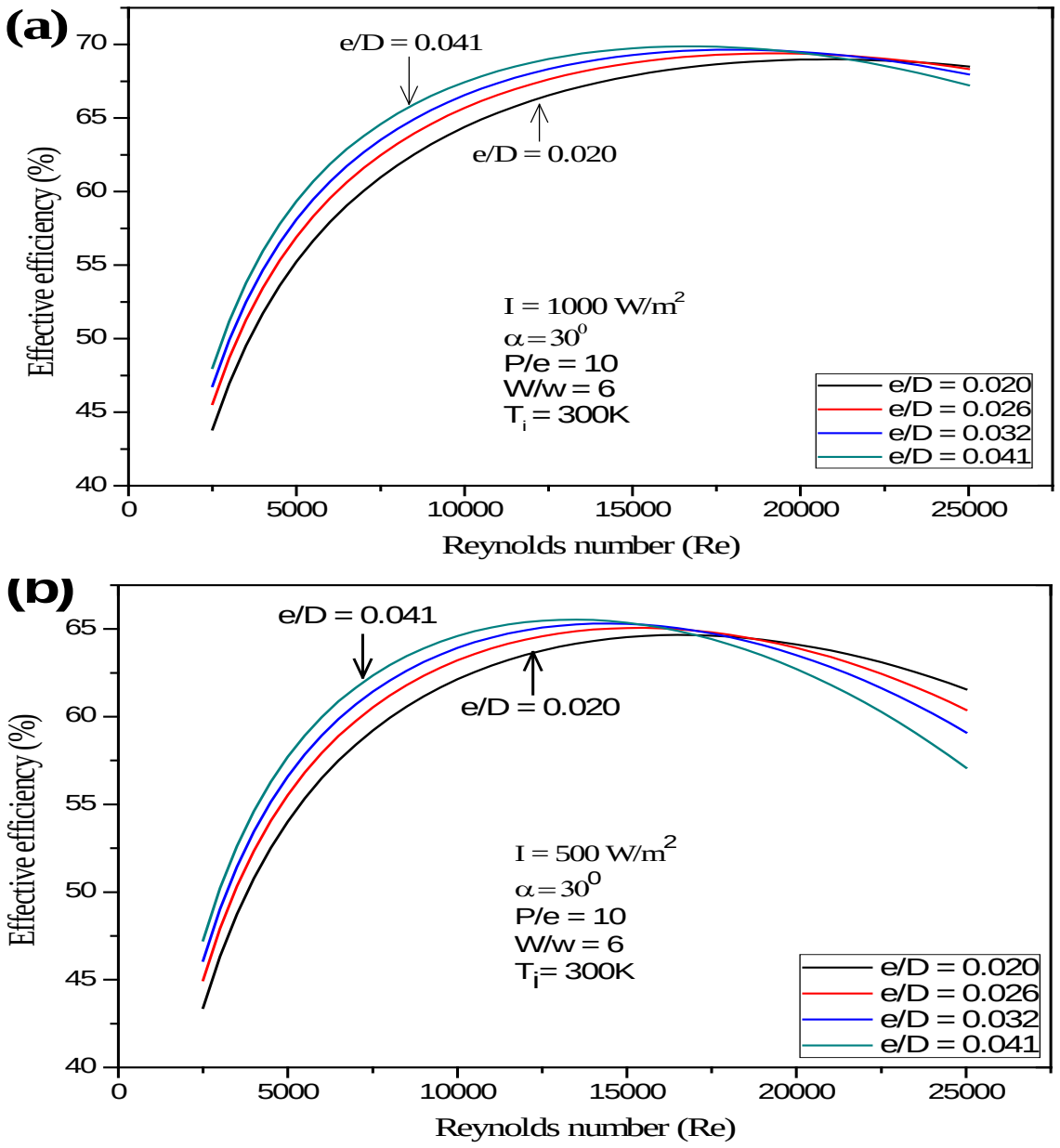

Fig. 4. Effect of relative roughness height on effective efficiency (a) Insolation (I) =1000 W/m^2 (b) Insolation (I) =500 W/m^2.

4.2. Effect of Angle of Attack (α)

The variation in effective efficiency with Reynolds number for different values of angle of attack ($\alpha = 30^{\circ}, 45^{\circ}, 60^{\circ}$ and 75°) for fixed value of relative roughness height (e/D =0.041), relative roughness width (W/w = 6) and relative roughness pitch (P/e = 10) at insolation (I) of 1000 W/m^2 and 500 W/m^2 as shown in Figures 5 (a) and (b), respectively. It is observed that from Figure 5(a) the effective efficiency increases with increases of Reynolds number first attains maximum at certain value of Reynolds number, and after that decreases with further increase in Reynolds number. There exists an optimum value of effective efficiency for a given roughness configuration. This effect shows that the Reynolds number is a strong parameter that affects the pumping power and thermal energy gain, thereby affecting the effective efficiency.

In order to investigate the behaviour of angle of attack on the effective efficiency of solar collector, the parameters are taken to be fixed value of relative roughness height (e/D), relative roughness pitch (P/e), relative roughness width (W/w) and insolation (I) as shown in Figure 5(b). It is observed that the value of angle of attack ($\alpha = 60^{\circ}$) results in highest thermohydraulic performance whereas at the angle of attack ($\alpha = 30^{\circ}$) it is the lowest for all values of Reynolds number Re < 15,000 and Re < 12,000 as indicated in Figures 5 (a) and (b), respectively.

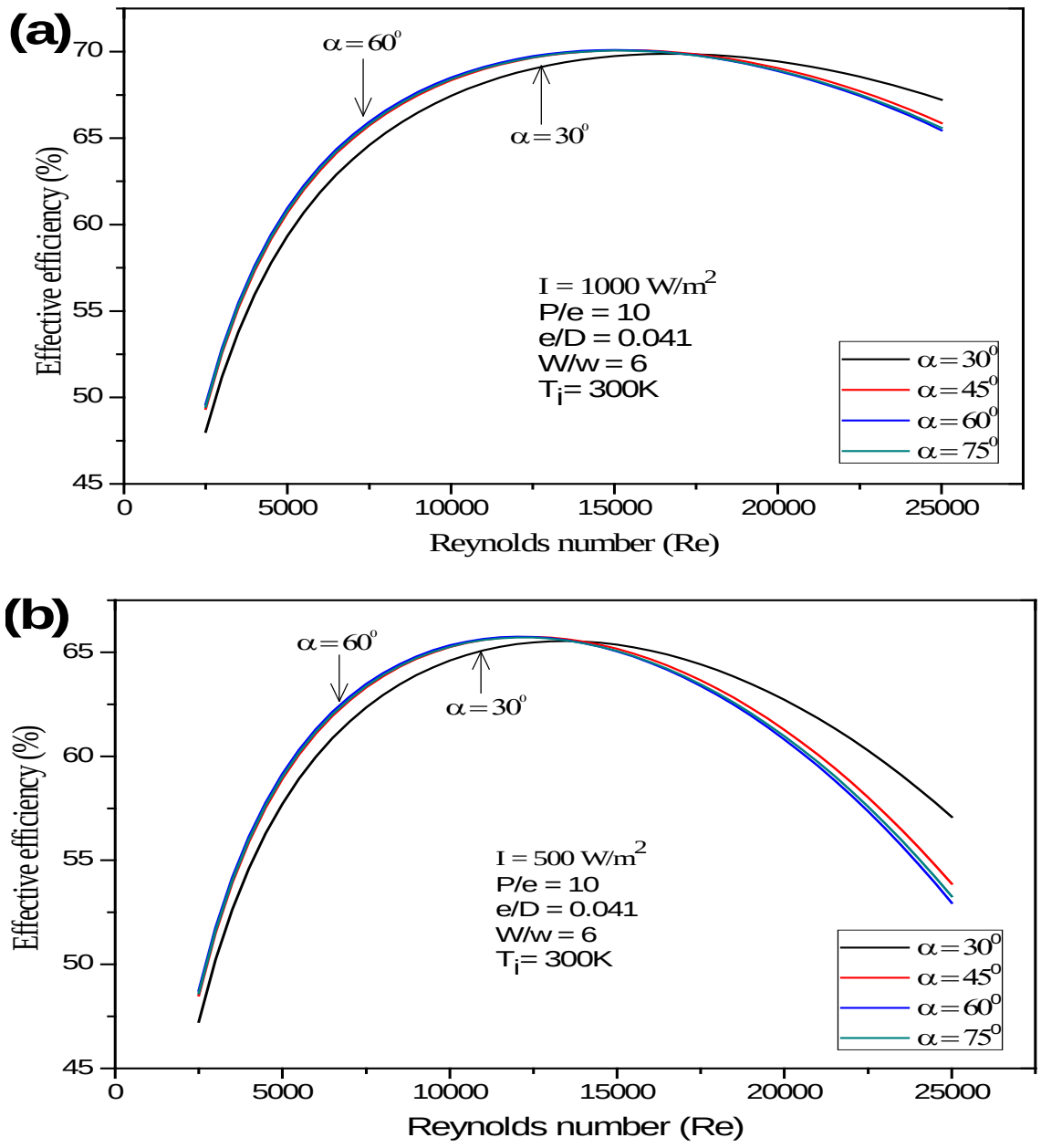

Fig. 5. Effect of an angle of attack on effective efficiency (a) Insolation (I) = 1000 W/m^2 (b) Insolation (I) = 500 W/m^2.

4.3. Effect of Intensity of Solar Radiation (I)

Figures 6 (a) and (b) shows the effective efficiency as a function of Reynolds number for different values of insolation. The selected values of roughness configuration and other parameters have been shown in these figures. It is found that for a particular value of insolation effective efficiency goes up to a maximum at a certain value of Reynolds number and after that it starts decreasing. The point corresponding to the maximum value of effective efficiency is found to shift to higher side of Reynolds number as the value of insolation increases. This leads to fact the flow rate of air through the duct should be adjusted to a Reynolds number such that the maximum effective efficiency for that value of insolation can be ensured. The effective efficiency increases with increase in insolation values. This appears due to increase in the absorber plate temperature with increase in insolation and leads to higher heat transfer rate to the air, pumping power remains unchanged.

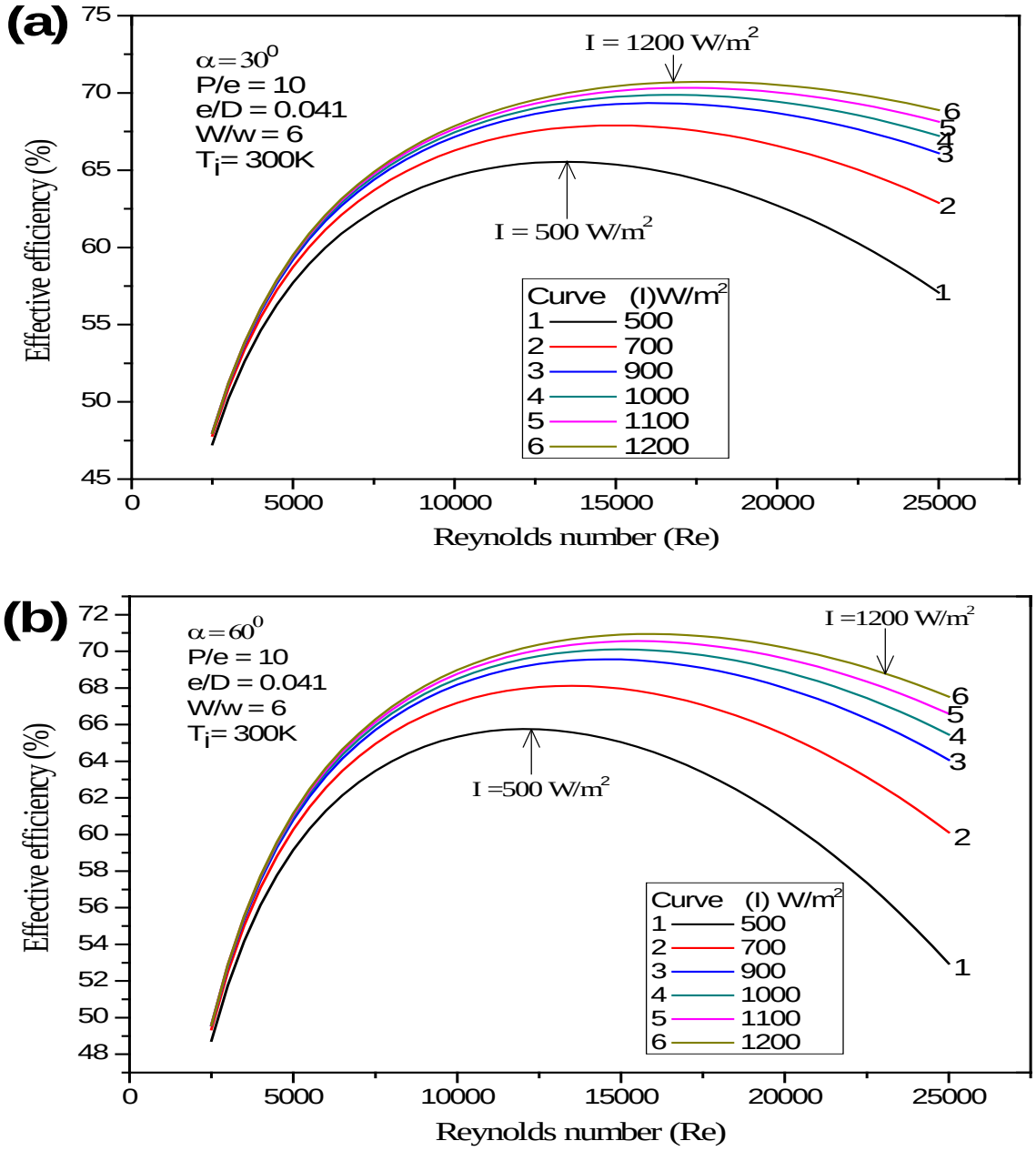

Fig. 6. Effect of solar radiation on effective efficiency (a) angle of attack of 30° (b) angle of attack of 60°.

Figures 7 (a) and (b) shows the variation of useful energy gain (Q_u) and thermal energy equivalent to the power consumption (Pm/ζ) as a function of Reynolds number for two values of insolation 1200 W/m^2 and 500 W/m^2. From Figure 7(a) it reveals that maximum value for the (Q_{net}) shifts to a lower range of Reynolds number as the insolation decreases and hence the point of maximum effective efficiency also shifted to a lower Reynolds number. The rate of increase of net energy gain (Q_{net}) is faster at higher value of insolation (I =1200 W/m^2) than that of the lower value of insolation (I =500 W/m^2). On the other hand in Figure 7(b) the pumping power (Pm/ζ) increases very slow rate with lower value of roughness Reynolds number ($e^+ < 70$) but increases rapidly in the higher value of roughness Reynolds number. This happens due to reduction in absorber plate temperature owing to low value of insolation and also due to lower mass flow rate of air that leads to decrease in rate of heat transfer to air in the duct, while the pumping power expenditure remains the same.

4.4. Effect of Reynolds number

Figure 8 shows the variation of effective efficiency with insolation for different values of Reynolds number for roughened solar air heater at constant values of relative roughness height, relative roughness pitch and angle of attack. The effective efficiency is observed to increase with insolation for all values of Reynolds number. However, in the range of Reynolds number 17,500 to 3500 it increases more rapidly as compared to other Reynolds number (Re < 17,500).

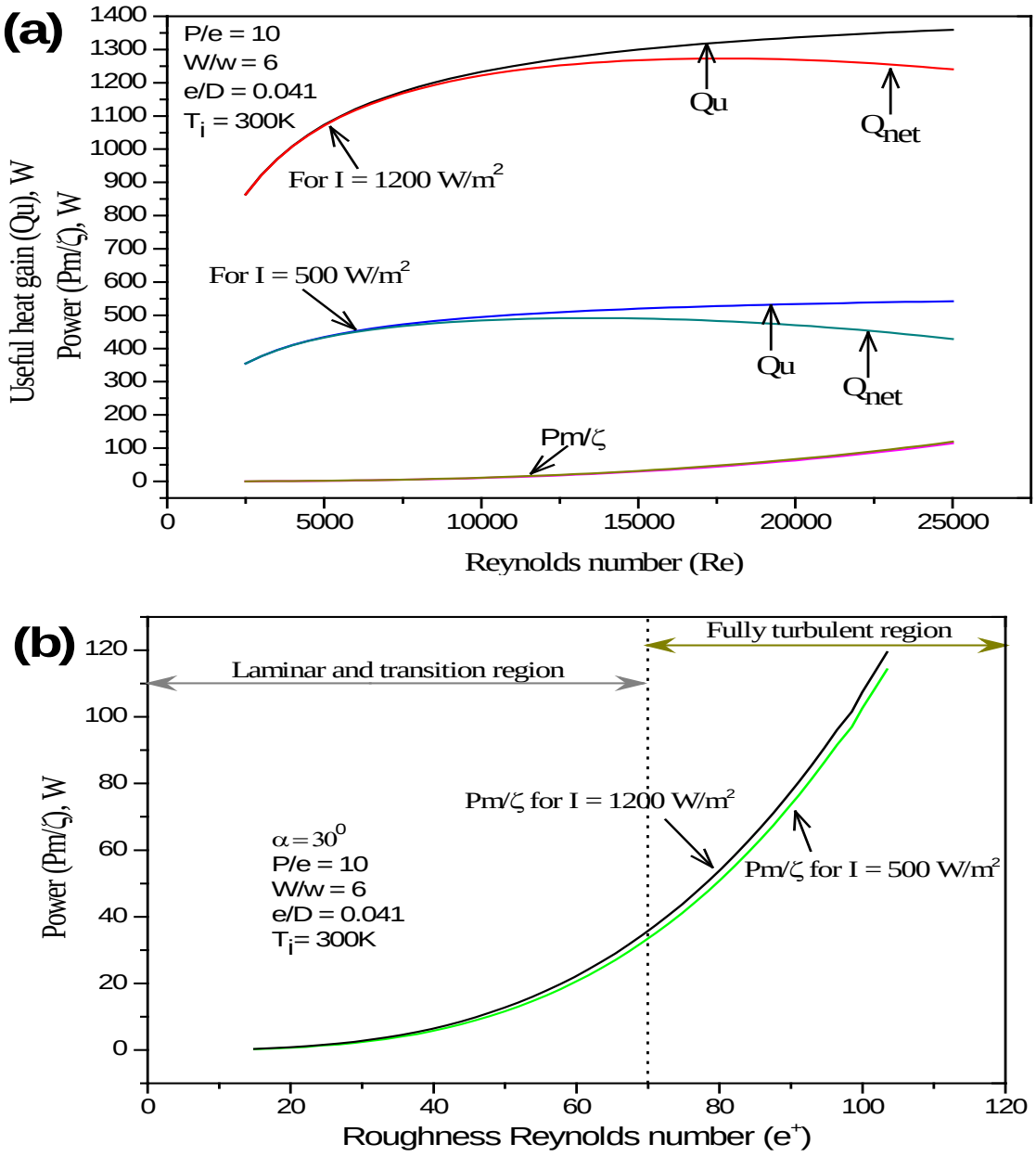

Fig. 7. (a) Useful energy and power consumption as a function of Reynolds number for different values of insolation (b) Enlarged view of Figure 7 (a) for (Pm/ζ).

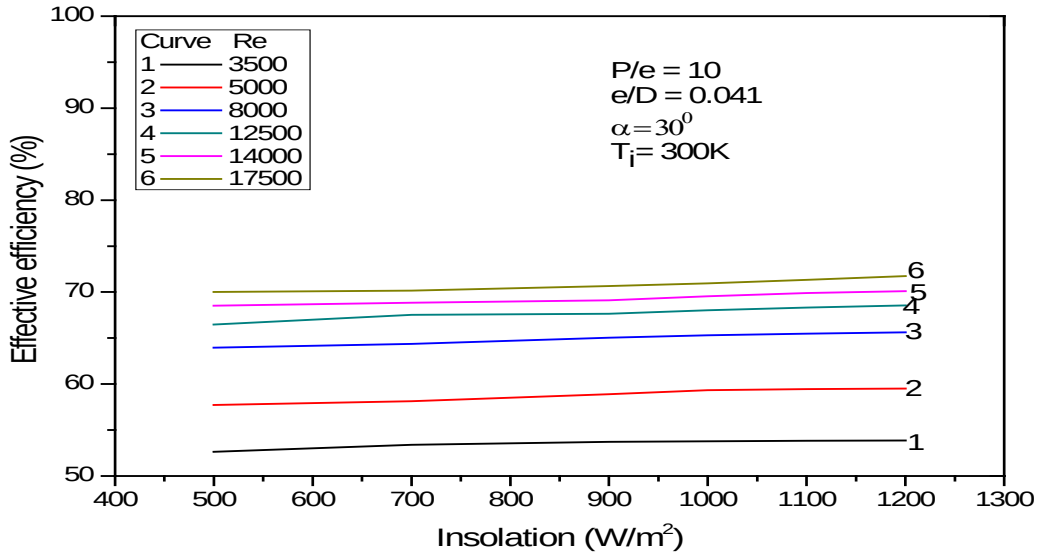

Fig. 8. Effective efficiency versus intensity of solar radiation for various values of Reynolds number.

4.5. Thermal and Effective Efficiency Comparison

Figures 9 (a) and (b) shows the thermal and effective efficiencies of multiple v-shaped roughened and smooth absorber plate solar air heater as a function of Reynolds number.

In Figure 9(a) the curves have been drawn for roughened solar air heater duct and are observed that the thermal efficiency increases continuously with Reynolds number, whereas the effective efficiency first increases, attains a maximum value and thereafter decreases with increase in Reynolds number. This trend of variation of effective efficiency indicates that the net thermal energy gain goes on decreasing after attaining its maximum value owing to increase in the equivalent energy gain against pumping power expended. Further, it can be attributed that there exists an optimum operating condition for a given configuration of roughness geometry at which the effective efficiency is maximum for a particular Reynolds number.

Figure 9(b) shows the comparison of thermal and effective efficiency for roughened and smooth solar air heaters as a function of roughness Reynolds number(e^+). It can be found that the thermal efficiency of rough as well as smooth solar air heaters increases continuously with all values of roughness Reynolds number(e^+). On the other hand effective efficiency of both solar air heaters increases in the transition region ($5 \leq e^+ \leq 70$) . The effective efficiency of roughened solar air heater attains its maximum value at roughness Reynolds number (e^+) of 74 (approx.) and after that it starts decreasing with increase in roughness Reynolds number, in case of roughened solar air heater. The effective efficiency of roughened solar air heater in fully developed turbulent flow region ($e^+ > 74$) , decreases, however it can be concluded that the use of roughness in the solar air heater is more beneficial as compared to smooth solar air heater up to a roughness Reynolds number of ($e^+ = 120$) from effective efficiency point of view.

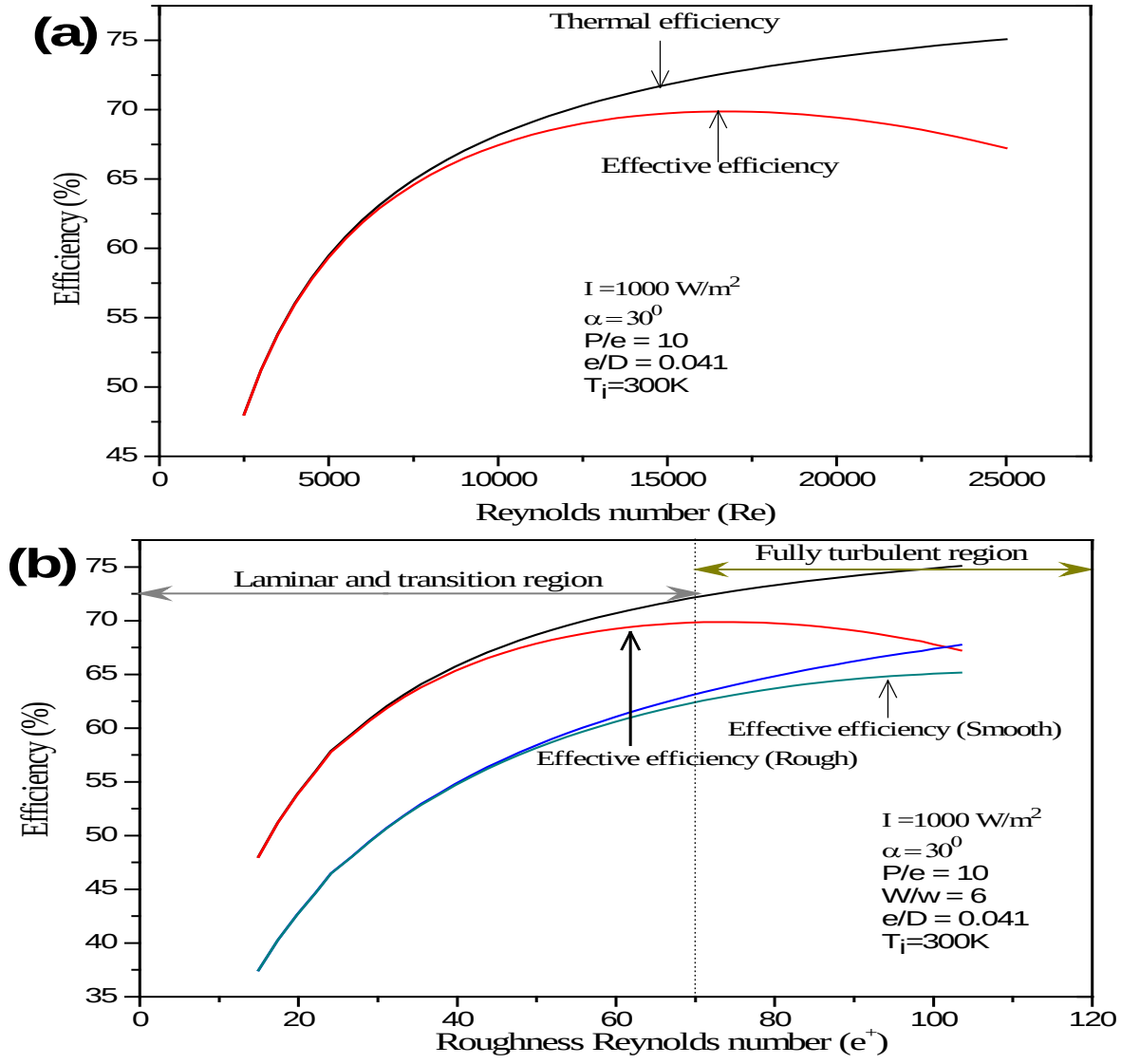

Fig. 9. (a) Thermal and effective efficiencies as a function of Reynolds number (b) Comparison of thermal and effective efficiencies for smooth and roughened solar air heaters.

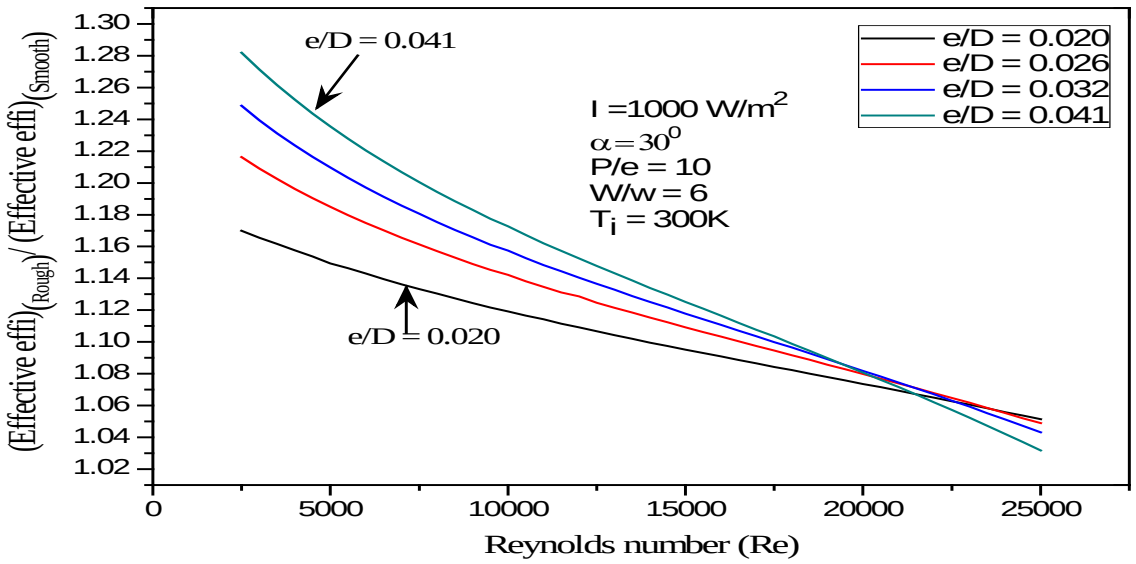

Fig. 10. Effective efficiency enhancement ratio of roughened to smooth solar air heaters versus Reynolds number for different values of relative roughness height.

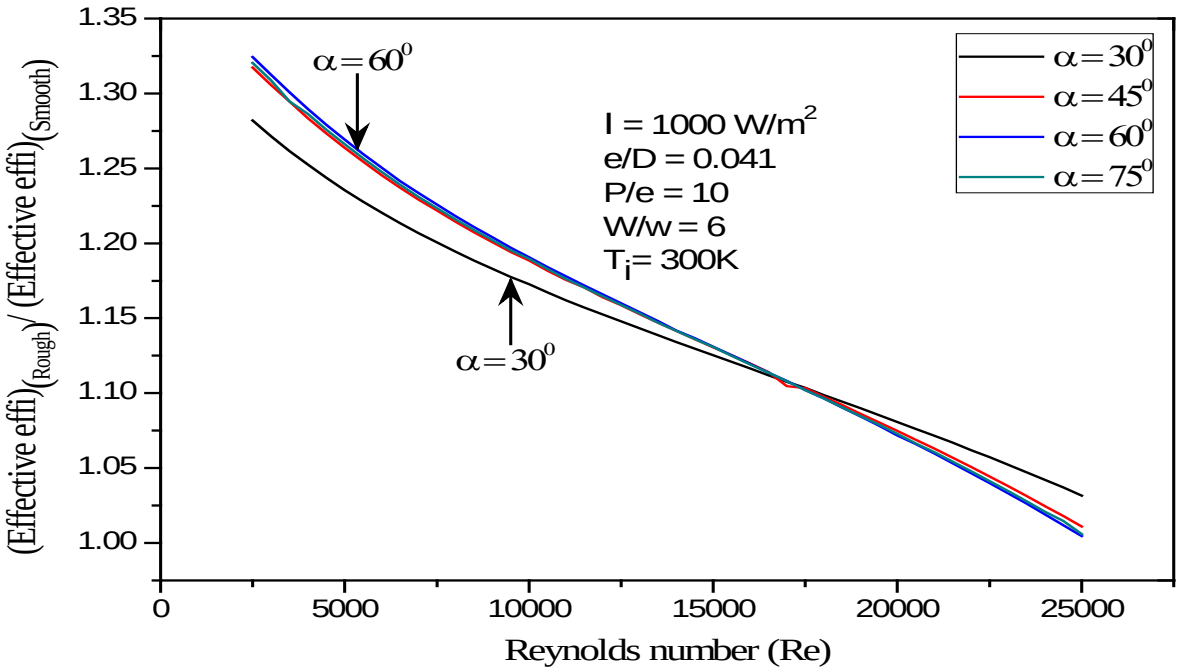

Fig. 11. Effective efficiency enhancement ratio of roughened to smooth solar air heaters versus Reynolds number for different values of angle of attack.

4.6. Variation of Enhancement Ratio (E_R)

The variation of effective efficiencies enhancement ratio of roughened to smooth solar air heater with the Reynolds number for different values of relative roughness height at insolation (I) = 1000 W/m^2, relative roughness pitch (P/e) = 10 and angle of attack (α) = 30^0 has been shown in Figure 10. It is found that the ratio (E_R) is highest for highest value of relative roughness height and is the lowest for lowest value of e/D; however this trend of variation for all values of e/D is the same. The Reynolds number corresponding to the maximum (E_R) shifts towards lower values of Reynolds number as e/D increases. In Figure 11 shows that the enhancement ratio of effective efficiencies verses Reynolds number for different values of angle of attack and fixed values of insolation, relative roughness heights, have been plotted. It is observed that effective efficiencies enhancement ratio is the highest for angle of attack(α) = 60° and lowest for (α) = 30° the nature of variation of effective efficiencies is same for all values of angle of attack.

4.7. Optimum Design Conditions

It has been observed that the point of maximum effective efficiency is a strong function of roughness parameters and insolation. The Reynolds number corresponding to optimum conditions also changes with roughness parameters and insolation. The performance of the roughened solar collectors have been prepared for the range of relative roughness height (e/D = 0.021 - 0.041), Reynolds number (Re = 2500 – 25,000) and insolation (I = 500 – 1200 W/m^2). In Figure 12 shows

that the variation of relative roughness height with Reynolds number for different values of insolation for optimum conditions and Figure 13 shows the relationship between the Reynolds number and solar insolation. It has been found that with increase in insolation, for a given relative roughness of height, Reynolds number that shows the maximum effective efficiencies, increases.

The following empirical equation has been developed based on these data (Table 2) that relates the system and operating parameters.

$$\mathrm{Re}_{\mathrm{optimal}} = 6.685 \times 10^2[(e/D)^{-0.2918}(I)^{0.3145})] \quad (32)$$

This equation correlates the data for optimum design conditions with a regression coefficient, R^2 = 0.996. It is recommended for use to determine the parameter values to achieve the maximum effective efficiency. The relationship between normalized roughness height and Reynolds number is shown in Figure 14.

Table 2. Optimum conditions.

e/D	Reynolds number					
	I = 1200 W/m^2	I = 1100 W/m^2	I = 1000 W/m^2	I = 900 W/m^2	I = 700 W/m^2	I = 500 W/m^2
0.020	19500	19000	18500	17800	16500	14700
0.026	18000	17500	17000	16500	15200	13700
0.032	16900	16600	16100	15500	14300	12900
0.041	15800	15400	15000	14500	13400	12100

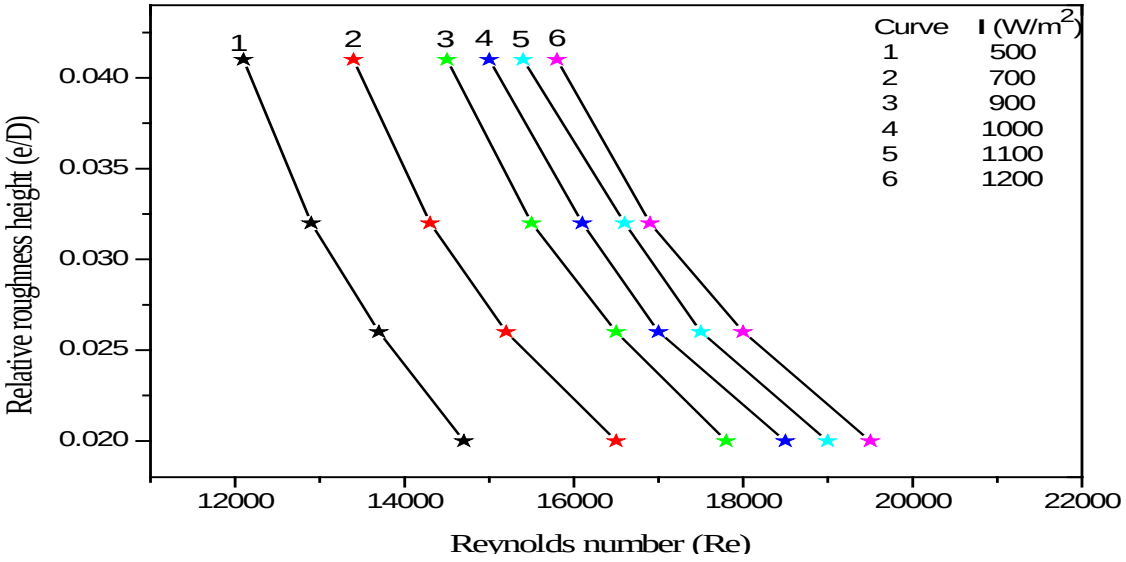

Fig. 12. Variation of relative roughness height with Reynolds number for optimum conditions of roughened solar air heater.

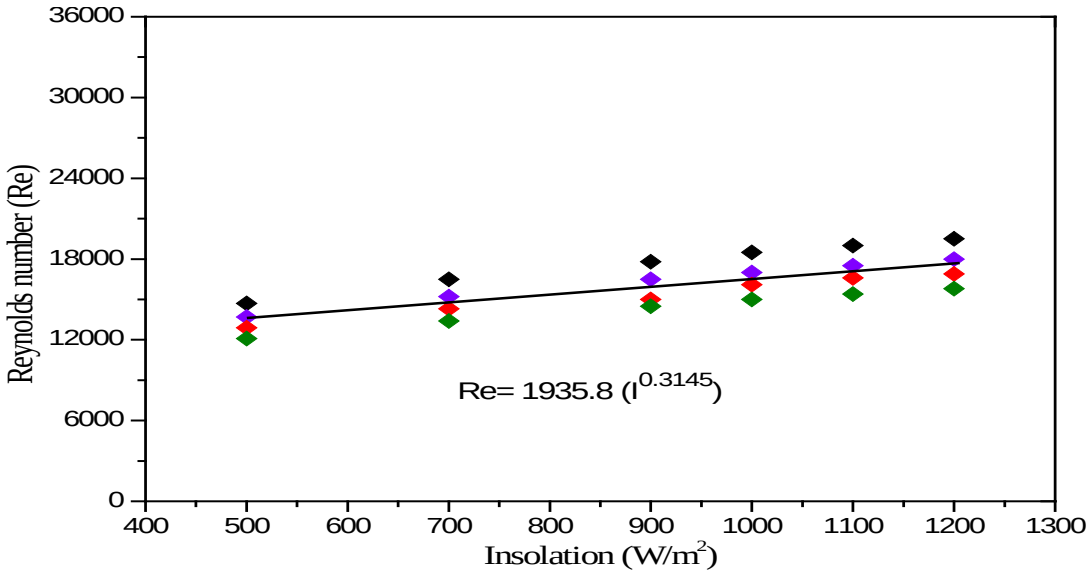

Fig. 13. Reynolds number versus intensity of solar radiation.

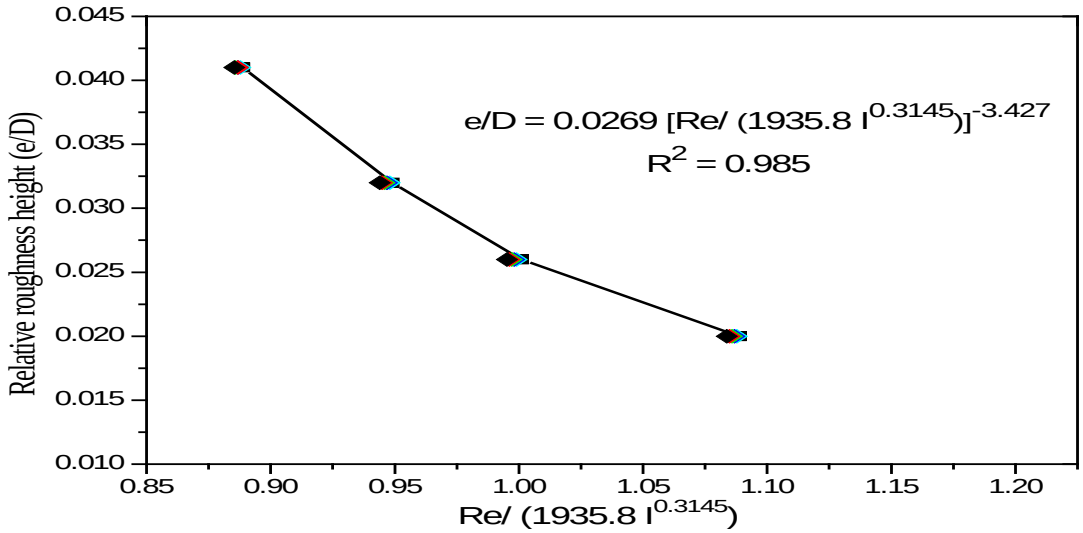

Fig. 14. Plots of $Re/(1935.8\ I^{0.3145})$ verses relative roughness height.

Table 3. Comparison of effective efficiency of solar collectors having multiple v-shaped wire rib roughness with other roughness geometries on the absorber plate.

Roughness Geometry and Author/s	Range of roughness parameters for evaluation	Correlations	
		Heat transfer (Nu)	Friction factor (f)
V-shape continuous ribs Momin *et al* [19]	P/e = 10 e/D = 0.041 Re = 2500-25000 $\alpha = 30^{\circ}$ I = 1000 W/m^2	$Nu_r = 0.067(Re)^{0.888}\left(\frac{e}{D}\right)^{0.424}(\alpha/60) - 0.077 \exp[-0.782(ln\alpha/60)^2]$	$f_r = 6.266(Re)^{-0.425}(e/D)^{0.565}(\alpha/60)^{-0.093}$
Combination of Inclined and Transverse ribs Varun *et al*. [23]	P/e = 10 Re = 2500-25000 I = 1000 W/m^2	$Nu_r = 0.0006(Re)^{1.213}(P/e)^{0.0104}$	$f_r = 1.0858(Re)^{-0.3685}(P/e)^{0.0114}$
Multigap V-down ribs combined with staggered ribs. Deo *et al*. [15]	P/e = 10 e/D = 0.041 Re = 2500-25000 $\alpha = 30^{\circ}$ I = 1000 W/m^2	$Nu_r = 0.02253(Re)^{0.98}(P/e)^{-0.06}(e/D)^{0.18}(\alpha/60)^{0.04}$	$f_r = 0.0371(Re)^{-0.15}(P/e)^{0.21}(e/D)^{0.65}(\alpha/60)^{0.57}$
Arc shaped wire ribs. Saini and Saini [24]	e/D = 0.041 Re = 2500-25000 $\alpha = 30^{\circ}$ I = 1000 W/m^2	$Nu_r = 0.00104(Re)^{1.3186}(e/D)^{0.3772}(\alpha/90)^{-0.1198}$	$f_r = 0.1440(Re)^{-0.17103}(e/D)^{0.1765}(\alpha/90)^{0.1185}$
Turbulator shape Bopche and Tanda [22]	P/e = 10 e/D = 0.041 Re = 2500-25000 I = 1000 W/m^2	$Nu_r = 0.5429(Re)^{0.7054}(p/e)^{-0.1592}(e/D)^{0.3619}$	$f_r = 1.2134(Re)^{-0.2076}(p/e)^{-0.4259}(e/D)^{0.3285}$
Multiple v- shaped wire rib roughness Present work	P/e = 10 e/D = 0.041 Re = 2500-25000 $\alpha = 30^{\circ}$ W/w = 6 I = 1000 W/m^2	$Nu_r = 3.35x10^{-5}(Re)^{0.92}(e/D)^{0.77}(W/w)^{0.43}(\alpha/90)^{-0.49}\exp[-0.1177(lnW/w)2]\exp[-0.61(ln\alpha/90)2](P/e)^{8.54}\exp[-2.0407(lnP/e)^2]$	$f_r = 4.47x10^{-4}(Re)^{-0.3188}(e/D)^{0.73}(W/w)^{0.22}(\alpha/90)^{-0.39}\exp[-0.52(\ln\alpha/90)^2](P/e)^{8.9}\exp[-2.133(lnP/e)^2]$

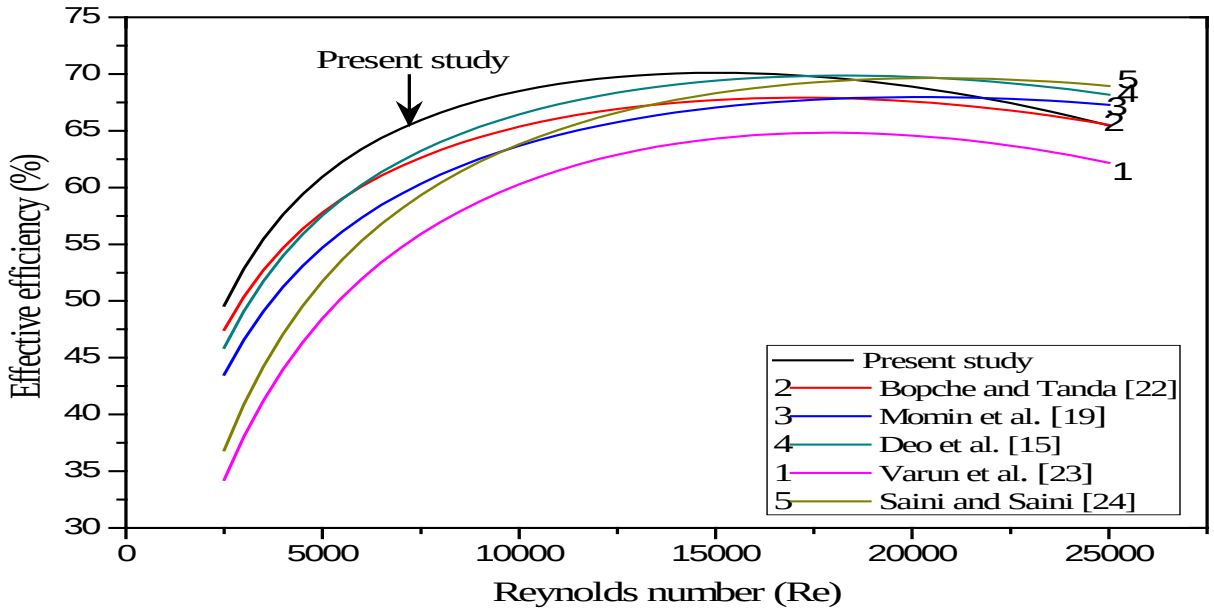

Fig. 15. Comparison of effective efficiency for multiple v-shaped wire rib roughness with other roughness geometries of roughened solar air heaters.

5. COMPARISION OF EFFECTIVE EFFICIENCY OF MULTIPLE V-SHAPED AND OTHER ROUGHNESS GEOMETRIES

Figure 15 show that the comparison of effective efficiencies of multiple v-shaped wire rib roughened solar air heaters, obtained in the present work with effective efficiencies of solar air heaters having other roughness geometries, for a common roughness and operating parameters, using the respective correlations as given in Table 3. It is found that every roughness geometries corresponds to an optimum value of effective efficiency of solar air heater corresponding to a particular Reynolds number however, it has the lower effective efficiency than the multiple v-shaped wire rib roughness (present work). All other roughness geometries have lower effective efficiency as compared to multiple v-shaped wire rib roughened solar air heater for all values of Reynolds number.

6. CONCLUSION

The following are the conclusions of the present investigation:

1. The rate of increase of useful energy gain is comparatively higher for roughened solar air heater at lower range of Reynolds number (Re < 13,000), whereas this rate of increase is lower at higher range of Reynolds number. The heat gain of roughened absorber plate is more as compared to smooth one for all values of Reynolds number.
2. The rate of increase of power consumption is low for lower range of Reynolds number (Re < 13000) and increases comparatively at high rate as Reynolds number increases (Re > 13000). Thermal efficiency increases with relative roughness height.
3. The values of insolation increases, the maximum values of effective efficiency shifts to higher Reynolds number. This leads to the conclusion that the flow should be adjusted to a Reynolds number so that maximum effective efficiency for that value of insolation is ensured.
4. Thermal and effective efficiency relatively increase up to transition region .Thermal efficiency increases continuously for roughened and smooth solar air heaters for all the values of Reynolds numbers, but effective efficiency for roughened solar air heater starts decreasing after attaining maximum value corresponding to a particulars Roughness Reynolds number.
5. The optimum design conditions for roughened solar air heaters have been determined for varying relative roughness height and insolation and for a relative roughness pitch of 10 for different angle of attack of roughness elements. The following empirical relationship relates the system and operating parameters that combine to yield the optimum conditions:

$$Re_{optimal} = 6.685 \times 10^2[(e/D)^{-0.2918}(I)^{0.3145})]$$

It is recommended for use to determine the parameter values to achieve the maximum effective efficiency.

NOMENCLATURE

A_c	Surface area of absorber plate, m^2
B	Solar air heater duct height, m
C_p	Specific heat of air at constant pressure, J/kg K
D	Equivalent or hydraulic diameter of solar air heater, D = 4WB/2(W+B), m
e	Roughness height, m
G	Mass velocity of air kg/sm^2
h	Convective heat transfer coefficient, W/m^2K
h_w	Wind convective heat transfer coefficient, W/m^2K

I	Intensity of solar radiation W/m^2
K	Thermal conductivity of air, W/m K
K_g	Thermal conductivity of glass cover, W/mK
K_i	Thermal conductivity of insulation, W/mK
L	Length of absorber plate, m
L_1	Spacing between absorber plate and glass cover, m
$\dot{m}$	Mass flow rate of air, Kg/s
N	Number of glass cover
P	Roughness pitch, m
P_m	Pumping power, W
$(\Delta P)_d$	Pressure drop across the duct, Pascal
T_i	Inlet temperature of air, K
T_o	Outlet temperature of air, K
T_a	Ambient temperature, K
$\overline{T}_p$	Mean plate temperature, K
$\overline{T}_f$	Bulk mean temperature of air, K
T_g	Temperature of glass cover, K
L_e	Thickness of collector edge, m
L_g	Thickness of glass cover, m
ΔT	(T_o-T_i) Air temperature rise across the duct, ℃
$(\Delta T/I)$	Temperature rise parameters ℃m^2/W
Q_u	Useful heat gain, W
U_b	Bottom loss coefficient, W/m^{2}K
U_L	Overall heat loss coefficient, W/m^{2}K
U_t	Top loss coefficient, W/m^{2}K
U_s	Side loss coefficient, W/m^{2}K
V_w	Wind velocity, m/s
V	Velocity of air in the duct, m/s
W	Width of duct, m
w	Width of single-v, m

Dimensionless parameters

E_R	Enhancement ratio
e^+	Roughness Reynolds number
f_r	Friction factor for rough duct
f_s	Friction factor for smooth duct
F'	Collector efficiency factor
F_R	Collector heat removal factor
W/B	Duct aspect ratio
Re	Reynolds number
P/e	Relative roughness pitch
Nu_s	Nusselt number for smooth duct
Nu_r	Nusselt number for rough duct
e/D	Relative roughness height

Greek symbols

μ	Dynamic viscosity of air, Ns/m^2
σ	Stefan'-Boltzmann's constant, W/m^2 K^4
ρ	Density of air, kg/m^3
α	Angle of attack, degree
ε_g	Emissivity of glass cover
ε_p	Emissivity of absorber plate
δ_i	Thickness of insulation, m
η_{eff}	Effective efficiency
η_f	Fan or blower efficiency
η_{tr}	Electrical power transmission efficiency
η_m	Efficiency of electric motor
η_c	Carnot efficiency
η_{th}	Thermal efficiency

REFERENCES

[1] Webb R.L. and E.R.G. Eckert. 1972. Application of rough surfaces of heat exchanger design. *International Journal of Heat Mass Transfer* 5: 1647-1658.

[2] Saini J.S., 2004.Use of artificial roughness for Enhancing Performance of Solar air heater. In the *Proceedings of XVII national and VI ISHME/ASME Heat and Mass Transfer Conference*, January 05-07, IGCAR, Kalpakkam, India.

[3] Han J.C., Glicksman L.R. and Rosenow W.M., 1978. Investigation of heat transfer and friction for rib- roughened surfaces. *International Journal of Heat Mass Transfer* 21: 1143-1156.

[4] Lau S.C., McMillin R.D. and Han J.C., 1991. Turbulent heat transfer and friction in a square channel with discrete rib turbulators. *Transactions of ASME, Journal of Turbo Machinery* 113: 360-366.

[5] Lau S.C., McMillin R.D. and Han J.C., 1991.Heat transfer characteristics of turbulent flow in a square channel with angled rib. *Transactions of ASME, Journal of Turbo Machinery* 113: 367-374.

[6] Han J.C. and J.S. Park. 1988. Developing heat transfer in rectangular channels with rib turbulators. *International Journal of Heat Mass Transfer* 3(1): 183-195.

[7] Han J.C., 1984. Heat transfer and friction characteristics in rectangular channels with two opposite rib- roughened walls. *ASME Journal Heat Transfer* 106: 774-781.

[8] Han J.C., Park J.S. and Lei C.K., 1985. Heat transfer enhancement in channels with turbulence promoters. *ASME Journal Engineering Gas Turbines Power* 107: 628-635.

[9] Wright L.M., Fu W.L. and Han J.C., 2004. Thermal performance of angled, V-shaped, and W-shaped rib turbulators in a rotating rectangular cooling channels. *(AR=4:1), ASME Transactions, Journal of Turbomachinary* 126: 604-614.

[10] Tslim M.E., Bondi L.A. and Kercher D.M., 1991. An experimental investigation of heat transfer in an orthogonally rotating channel with 45 deg criss-cross ribs on two opposites walls. *ASME Journal Turbomachinary* 113: 346-353.

[11] Tslim M.E., Li T. and Kercher D.M., 1996. Experimental heat transfer and friction in channels roughened with angled V- shaped and discrete ribs on two opposites walls. *ASME Journal Turbomachinary* 118: 20-28.

[12] Gao X. and B. Sunden. 2001. Heat transfer and pressure drop measurements in rib roughened rectangular ducts. *Experimental Thermal and Fluid Science* 24(1-2): 25-34.

[13] Prasad K. and S. Mullick. 1983. Heat transfer characteristics of a solar air heater used for drying purposes. *Applied Energy* 13: 83-93.

[14] Prasad B.N. and J.S. Saini. 1988. Effect of artificial roughness on heat transfer and friction factor in solar air heater. *Solar Energy* 41: 555-560.

[15] Deo N.S., Chander S. and Saini J.S., 2016. Performance analysis of solar air heater duct roughened with multigap V-down ribs combined with staggered ribs. *Renewable Energy* 91: 484-500.

[16] Karmare S.V. and A.N. Tikekar. 2009. Experimental investigation of optimum thermohydraulic performance of solar air heaters with metal rib grits roughness. *Solar Energy* 83: 6–13.

[17] Karwa R., Solanki S.C. and Saini J.S., 2001. Thermohydraulic performance of solar air heaters having integral chamfered rib roughness on absorber plates. *Energy* 26: 161–176.

[18] Nikuradse J., 1950. Laws for flow in rough pipes. *National Advisory Committee for Aeronautics:* NACA *Technical Memorandum* 1292.

[19] Momin A.M.E., Saini J.S. and Solanki S.C., 2002. Heat transfer and friction in solar air heater duct with V-shaped rib roughness on absorber plate. *International Journal of Heat Mass Transfer* 45: 3383–3396.

[20] Prasad B.N., Behura A.K. and Prasad L., 2014. Fluid flow and heat transfer analysis for heat transfer enhancement in three sided artificially roughened solar air heater. *Solar Energy* 105: 27–35.

[21] Prasad B.N., Kumar A. and Singh K.D.P., 2015. Optimization of thermo hydraulic in three sides artificially roughened solar air heaters. *Solar Energy* 111: 313–319.

[22] Bopche S.B. and M.S. Tandale. 2009. Experimental investigations on heat transfer and frictional characteristics of a turbulator roughened solar air heater duct. *International Journal of Heat and Mass Transfer* 52: 2834–2848.

[23] Varun, Saini R.P. and Singal S.K., 2008. Investigation of thermal performance of solar air heater roughness elements as a combination of inclined and transverse ribs on absorber plate. *Renewable Energy* 33: 1398-1405.

[24] Saini S.K. and R.P. Saini. 2008. Development correlations for Nusselt number and friction factor for solar air heater with roughened duct having arc-shaped wire as artificial roughness. *Solar Energy* 82: 1118–1130.

[25] Cortes A. and R. Piacentini. 1990. Improvement of efficiency of a bare solar collector by means of turbulence promoter. *Applied Energy* 36: 253–261.

[26] Duffie J.A. and W.A. Beckmen. 1980. Solar Engineering of Thermal Processes. New York: Wiley.

[27] Duffie J.A. and W.A. Beckmen. 1991. Solar Engineering of Thermal Processes. 2nd edition, John Wiley, New York.

[28] Hans V.S., Saini R.P. and Saini J.S., 2010. Heat transfer and friction factor correlations for a solar air heater duct roughened artificially with multiple v-ribs. *Solar Energy* 84: 898-911.

[29] Malhotra A., Garg H.P. and Palit A., 1981. Heat loss calculation of flat plate solar collectors. *Journal of Thermal Energy* 2, pp. 2.

[30] Gupta D., Solanki S.C. and Saini J.S., 1997. Thermo-hydraulic performance of solar air heaters with roughened absorber plates. *Solar Energy* 61(1): 33–42.

[31] Singh S., Chander S. and Saini J.S., 2012. Investigations on thermo-hydraulic performance due to flow-attack angle in v-down rib with gap in rectangular duct of solar air heater. *Applied Energy* 97: 907–912.

[32] Kumar A., Saini R.P. and Saini J.S., 2013. Development of correlations for Nusselt number and friction factor for solar air heater with roughened duct having multi v-shaped with gap rib as artificial roughness. *Renewable Energy* 58: 151-163.

[33] Karwa R. and G. Chitoshiya. 2013. Performance studyof solar air heater having v-down discrete ribs on absorber plate. *Energy* 55: 939-955.